Electrospun composite fiber for liquefied petroleum gas sensing

T. Victoria Adeseluka [1,5], S. Oluwagbemiga Alayande [2] *, Emmanuel Ajenifuja [3], F. Joke Okparaocha [4], O. Fasakin [1], J. Adegbindin Ajao [3]

[1] *Department of Physics and Engineering Physics, Obafemi Awolowo University, Ile Ife, Nigeria*
[2] *Department of Industrial Chemistry, First Technical University, Ibadan, Nigeria*
[3] *Centre for Energy Research and Development, Obafemi Awolowo University, Ile Ife, Nigeria*
[4] *Department of Science Laboratory Technology, Federal College of Agriculture, Ibadan, Nigeria*
5. *Department of Physics, Bingham University, Nassarawa, Nigeria.*
*Corresponding author E-mail: samson.alayande@tech-u.edu.ng

Abstract

Advancement in the volume of waste generated from polymers demands innovation on its' management and re-use strategy. In this study, advance materials technique was used for polymeric wastes management, namely expanded polystyrene (EPS), discarded compact discs (polycarbonate (PC), these were electrospun with polyaniline (PANI) and zinc oxide (ZnO) to produce fibrous scaffolds. The fibrous scaffolds were characterized using Fourier Transform Infrared spectrometer (FTIR), Scanning Electron Microscopy (SEM), X-ray diffractometer and Differential Thermal Analysis (DTA). Due to it Ohmic property, resistivity sensing potential was explored for Liquefied Petroleum Gas (LPG). The fibre exhibited high sensitivity and short response time towards LPG at room temperature. This work presents a sustainable, affordable and effective pathway for re-using polymeric wastes as potential resistivity gas sensor.

Keywords: *Polymeric Wastes; Polymer Nanocomposite; Fibrous Scaffolds; Sensitivity; Liquefied Petroleum Gas.*

1. Introduction

Polymeric materials have notable properties, namely excellent mechanical properties, low density, durability and low cost, supporting wide usage in our contemporary daily lives. However, due to the persistence of these materials in the environment, they can be intentionally or inadvertently released into the environment as wastes and therefore presents danger to our ecosystems [1]. Globally, studies have shown that besides food and paper waste, polymeric waste is the third major constitute at municipal and industrial waste in cities [2]. Prominent among polymeric wastes are polycarbonate (discarded compact discs), expanded polystyrene (EPS), polyethylene (pure water sachet) and polyethylene terephthalate (PET bottle) [2]. These wastes have been recycled using several approaches such as chemical, mechanical, material, craft, etc [2]. These processes do not result to re-use in a pathway that is sustainable.

Notable is material recycling technique, valuable tool for solid waste management [2]. For instance, our previous efforts using this concept for re-use of expanded polystyrene had resulted to advanced superhydrophobic-superoleophillic sorbents for petroleum fingerprinting [3,4]; superoleophillic adsorbents [3-6] and porous electrospun membranes [7,8]. One of the techniques for material recycling is electrospinning [2,7,8], resultant fibres are classified advance materials due to high surface area to volume ratio and dimension. Through this mechanism, conducting fibrous scaffold have being fabricated, either based on a blend of conducting fillers and insulating polymer or vice versa. Conducting polymers are materials that can transmit electrical charges just like inorganic metals and semiconductors. It has non-corrosive, easy synthesis, flexibility, electrical and structural diversity properties [9]. Amongst the family of conducting polymers, polyaniline (PANI) is one of the most promising electrically conducting polymers due to its unique electrical, electrochemical properties, easy polymerization, high environmental stability and low cost of monomer [10]. It is widely used in applications such as microelectronic devices, diodes, light weight batteries, sensors, super capacitors, microwave absorption, corrosion inhibition [10]. Limitations such as lack of consistency and low electrical conductivity provoked development of composite conducting polymers. This development has been based either structural modification or incorporation of conducting heterogenous materials such as nanomaterials, quantum dots, etc with conducting polymers. These have enhanced resultant materials selectivity and sensitivity.

Besides, gas sensing devices based on conducting polymers, such as polypyrrole, polyaniline, and metaphthalocyanines, are notable for high sensitivity at room temperature, but their long response time due to the orderly structure limits their usage [11-13]. Therefore, incorporation of metal oxide semiconductors (MOS) nanoparticles into the polymer solution to generate functional nanocomposite fibres improves sensing sensitivity, conductivity and gives short response time due to their high surface area and small dimensions [13-16]. The enlarged surface area enhances the interactions between the materials and analytes, which leads to high sensitivity and the small dimensions, facilitate adsorption/desorption kinetics for analytes in the materials, which allows a rapid response time and high signal reproducibility

[17]. Metal oxide semiconductors (MOS) nanoparticles, such as zinc oxide nanoparticles; have long been used for sensing purposes based on conductivity and/or impedance change [18].

Considering the importance of sensors in many areas such as environmental monitoring, industrial process control, medical diagnosis, toxic chemical detection, etc. It is crucial to develop affordable sensors particularly for specialized applications in developing and under-developing nations. While properties such as sensitivity, selectivity, and reliability will not be compromised. To achieve this feat, polymeric wastes can be blended with conducting polymer and semiconductor material based on versatile nature of electrospinning techniques. Resultant conducting fibre will present sustainable path to re-use polymer wastes, monitor gases and reduce cost of conventional sensor. In this work, discarded compact disc (Polycarbonate), expanded polystyrene (EPS), polyaniline and zinc oxide (ZnO) were electrospun to fibre as potential gas sensor for liquefied petroleum gas sensing.

2. Experimental section

2.1. Materials reagents

The reagents: acetone, aniline, ammonium persulphate (APS), distilled water, methanol, deionized water, zinc nitrate hexahydrate ($ZnNO_3.6H_2O$), sodium hydroxide (NaOH) pellets, ethanol and dichloroethane (DCE), all purchased from Sigma-Aldrich.

2.1.1. Synthesis of polyaniline (PANI) doped with formic acid

Polyaniline was synthesized by a chemical method in the formic acid medium using ammonium persulphate (APS) as oxidizing agent and aniline as reagents as previously reported by Yue et al., [19].

2.1.2. Synthesis of zinc oxide nanoparticles

Zinc oxide nanoparticle was also synthesized using the sol-gel method in which zinc nitrate was the precursor and sodium hydroxide pellets used as the reducing agent as reported by Becheri et. al., [20].

2.1.3. Electrospinning of pc and composites

15 w.t% of composites of PC, PC/EPS, and PC/EPS/PANI solutions were dissolved in 30 mL dichloroethane (DCE) and stirred for 3 hours using a magnetic stirrer. The solutions were electrospun to obtain fibres. Also, 5% of ZnO nanoparticles was dispersed in PC/EPS/PANI solution to form PC/EPS/PANI/ZnO and stirred using a magnetic stirrer for 3 hours. The sample was also electrospun using 1 mL syringe (spinneret) with a needle having an inner diameter of 0.4 mm tilted at 10º to maintain a droplet of the solution at the tip of the spinneret [2-7]. A clamp connected with high voltage power supplier, which can supply positive voltage from 0 to 30 kV, was attached to the needle. The positive terminal of the high voltage power supplier was dipped into the polymer solution for electricity to be conducted through the solution and the negative terminal attached to the aluminium foil collector. The polymer jets generated from the needle by high voltage flew to the grounded collector and formed the scaffolds. The distance between the needle tip and the aluminium collector was fixed at 15 cm and a critical voltage value of 18 kV was used. All these experiments took place under controlled atmospheric conditions at 25 ± 2 ºC and 35 ± 4% relative humidity.

2.2. Characterisation

The prepared PANI, ZnO NPs and the scaffolds were analyzed using a Fourier Transform Infrared (FTIR) spectrometry (Shimadzu FTIR 8300 series). The structure of ZnO NPs and the scaffolds were determined by X-ray diffractometer (XRD). A wavelength (λ) 0.15418 nm was used for these analyses. The XRD patterns were recorded at the scan speed of 2° min^{-1} between 2θ angles of 8º and 90º, where θ is the angle of incidence of the X-ray beam. SEM was applied to observe the surface morphology of ZnO NPs and the scaffolds (PC, EPS, PC/EPS, PC/EPS/PANI, PC/EPS/PANI/ZnO nanocomposites) using a Hitachi S4160 scanning electron microscope (SEM) at an acceleration voltage of 5 kV. The thermal properties of the samples were studied using Differential Thermal Analysis (DTA) NETZSCH model 404PC.

2.2.1. Gas sensing experiment

The response of the conducting formulation was tested for liquefied petroleum gas (LPG) at a temperature between 16-50 ºC using laboratory built up sensing apparatus. The LPG was purchased from Firstline Gas Company, Nigeria, in a sealed cylinder. The gas was then pumped by an in-line pump and guided through a Teflon pipe to the gas chamber. The nanocomposite fibre was placed into the glass chamber and gently pressed by two-probe. The initial resistance of the fibre was allowed to stabilize and measured before it was exposed to gas. The signal was produced and transfers to a computer system which measures the temperature as a function of time. The resistive sensitivity of the fibre was calculated using equation 1 (Nemade et al., 2010) in which Rg and Ra represents the resistance in test gas and dry air, respectively.

$$S (\%) = [(Ra - Rg)/Ra] \times 100\% \tag{1}$$

3. Results and discussion

3.1. FT-IR analysis

The molecular vibrations of polyaniline (PANI), zinc oxide (ZnO) nanoparticles, EPS and composite fibres (PC/EPS, PC/EPS/PANI, PC/EPS/PANI/ZnO) were determined from the FTIR spectra as shown in Figures 1-6. The FTIR spectrum of polyaniline (Figure 1) shows bands with the maximum in 1558 cm^{-1} and 1488cm^{-1} which is assigned to stretching vibrations of a quinoid ring (Q) and benzenoid (B)

ring respectively. The ratio of the maximum intensity of these two bands (I_Q/I_B) can be used to estimate the degree of oxidation on the polyaniline.
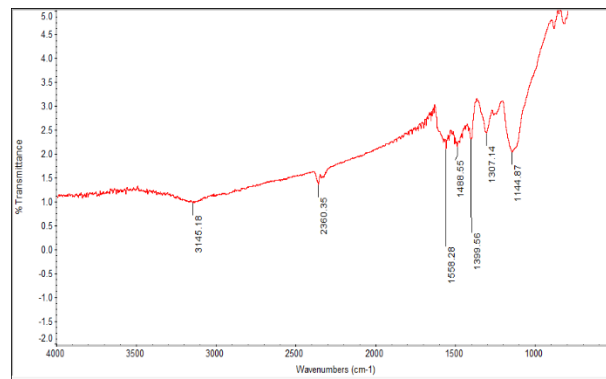
Fig. 1: FTIR Spectrum of Polyaniline.
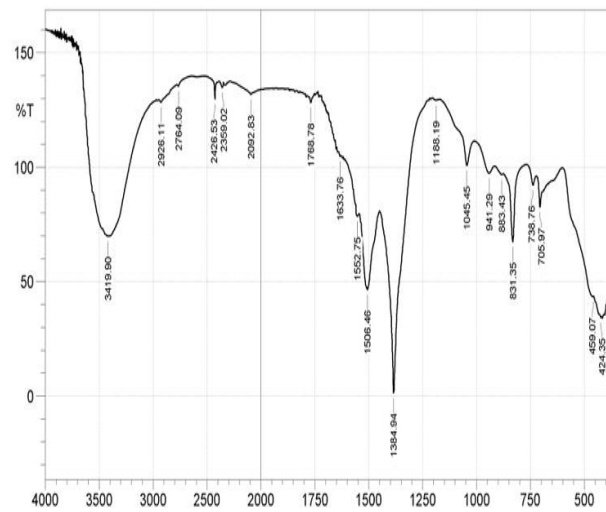
Fig. 2: FTIR Spectrum of ZNO NPS.
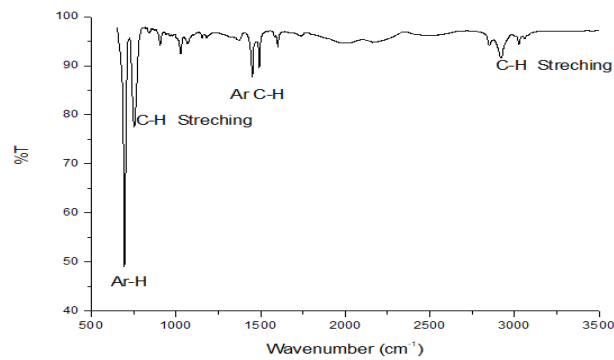
Fig. 3: FTIR Spectrum of Pure EPS.
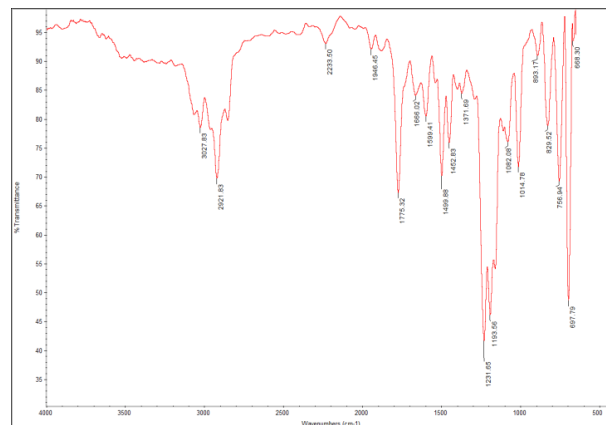
Fig. 4: FTIR Spectrum of Electro Spun PC/EPS.
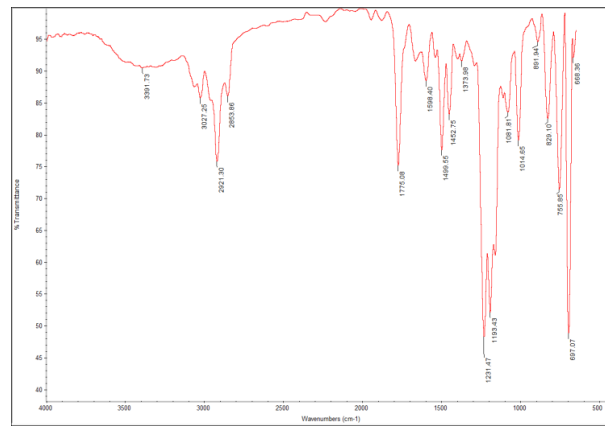
Fig. 5: FTIR Spectrum of PC/EPS/PANI.
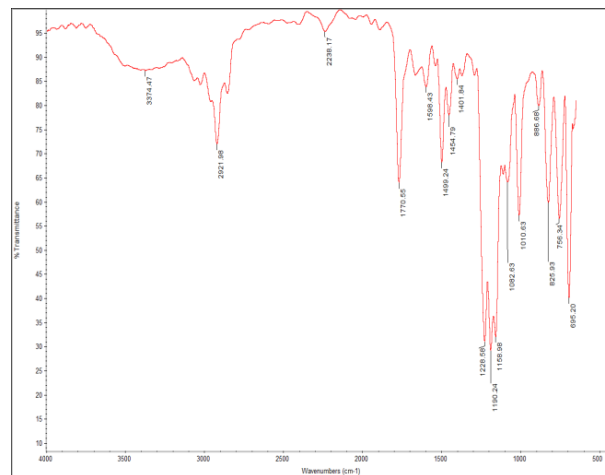
Fig. 6: FTIR Spectrum of PC/EPS/PANI/ZNO.

The band at 3145cm^{-1} is attributed to vibration of the NH$^+$ structure formed in the acid doping process of polyaniline and the band at 1307 cm^{-1} corresponds to C-N stretching vibrations. Figure 2 shows the FTIR spectrum of ZnO nanoparticles. Metal oxides generally give absorption bands in fingerprint region i.e. below 1000 cm^{-1} arising from inter-atomic vibrations. The peaks at λ = 459 and 424 cm^{-1} are related to the stretching vibrations of Zn-O bonds . A series of absorption peaks from 1000 to 4000 cm^{-1} can be found, corresponding to the carboxylate and hydroxyl impurities in materials. The peak at 3419 cm^{-1} indicates the presence of –OH residue, probably due to atmospheric moisture [20]. The peak at 2926 cm^{-1} are due to C-H stretching vibration of alkane groups. The peaks observed at 1633 and 1384 cm^{-1} are due to the asymmetrical and symmetrical stretching of zinc carboxylate respectively, carboxylate probably comes from reactive carbon-containing plasma species during the synthesis. The FTIR spectra of EPS and fibres (PC/EPS, PC/EPS/PANI and PC/EPS/PANI/ZnO) are shown in Figures 3 - 6. The spectra of the PC/EPS blends are quite similar to each other that are PC/EPS, PC/EPS/PANI and PC/EPS/PANI/ZnO nanocomposites show almost the same characteristic peaks. However, there is an evidence of peak displacement when PANI and ZnO nanoparticles are added to the PC/EPS.

FTIR spectrum of pure EPS fibre is shown in Figure 3. The molecular vibration observed at 3026 cm^{-1} indicates C-H stretching vibrations in the aromatic ring of polystyrene, peak at 1452 cm^{-1} corresponds to CH$_2$ bending vibration within the polystyrene ring. The peak at 2920 to 2848 cm^{-1} denotes C-H (alkyl group) symmetric and asymmetric vibration, peak at 1600 cm^{-1} shows aromatic ring-breathing modes of a benzene ring in polystyrene (PS).

In Figures 3 and 4, observed peak at 3027 cm^{-1} corresponds to the C-H stretching of an aromatic ring of polystyrene. The observed peaks at 3391 and 3374 cm^{-1} in Figure 5 and Figure 6 corresponds to the N-H stretching in polyaniline indicating the formation of PANI in the composites. Bending vibrations of out-of-plane C-H bonds of aromatic ring was observed at 755-695 cm^{-1}. This shows that the molecular structure of the polystyrene and polycarbonate blend remain intact despite the addition of zinc oxide nanoparticles and polyaniline. PC/EPS, PC/EPS/PANI and PC/EPS/PANI/ZnO fibre existed as the composite material. Figures 4 - 6, notable shift in wavelength number was observed in the relative intensity bands of polycarbonate (PC) at 1775, 1775 and 1770 cm^{-1} which correspond to carbonyl stretching of carbonate functional group. Also, shift in wavenumber was observed in the peak at 1599, 1598 and 1598 cm^{-1} which corresponds to C=C stretching vibration bond of benzene ring in polystyrene (PS). The molecular vibration observed at 893, 891 and 888 cm^{-1} corresponds to the C–CH$_3$ stretching (Lee et al., 2000). A shift in wavenumber was also observed in Figures 5 – 7 at 1452, 1452 and 1454 cm^{-1} which correspond to the CH$_2$ bending vibration of polystyrene.

3.2. Structural studies (X-ray diffraction)

ZnO nanoparticles, PC/PANI, PC/EPS, PC/EPS/PANI and PC/EPS/PANI/ZnO were studied structurally using XRD; results are presented in Figures 7-9. Figure 7 shows XRD pattern of ZnO nanoparticles. The sharp diffraction peaks apparent in figure 7 indicate good crystallinity of the ZnO nanoparticles. The diffraction peaks at 2θ = (31.77^0), (34.4^0), (36.2^0), (47.5^0), (56.6^0), (62.8^0) and (67.9^0); to the (100), (002), (101) and (102), (110), (103), (200), (112) diffraction planes, respectively, ascribed to the hexagonal structure of ZnO, these were in agreement with that of the typical wurtzite structure ZnO (hexagonal phase, space group P63mc, lattice parameters a = 3.24982, c = 5.20661 and JCPDS no. 36-1451). The average crystallite size of the zinc oxide was estimated from the full width at half maximum (FWHM) of the most intense peaks using Debye-Scherer equation; was found to be 21.1 nm.

Figure 8 shows the XRD pattern of the electrospun samples. From the result, all the XRD patterns are diffuse in shape which is an indication of amorphous nature of polymers. Electrospun PC and PC/PANI shows single diffuse XRD peak centered at $2\theta \sim 17.2°$ which is due to interference between the chains. The characteristic peak of PANI was observed at $2\theta = 25.45°$ corresponding to (2 0 0) crystal planes of PANI. PANI has a weak broad peak at $2\theta = 25°$, because of its amorphous structure with low crystallinity. No peaks corresponding to ZnO nanoparticles were observed. It may be due to very small mass percentage of ZnO nanoparticles dispersed on the surface of the fibre. Also, an addition of nanofiller tends to decrease the crystallinity of polymer matrix while amorphous phase increases accordingly (Li et al., 2005). The on-set of crystallinity in the electrospun fibres confirm nanostructuring of PC from its primary form.
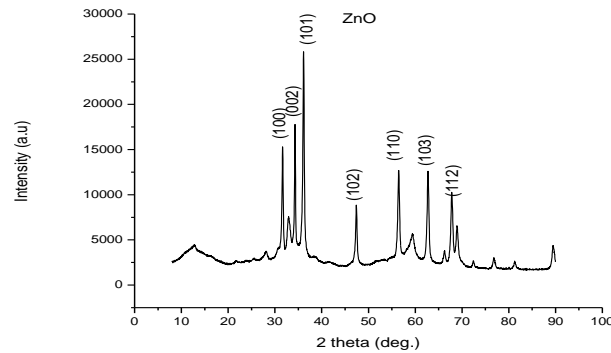
Fig. 7: XRD Pattern of Zno Nanoparticles.
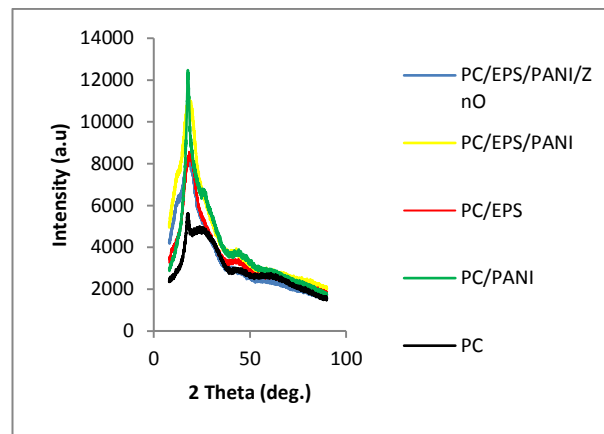
Fig. 8: XRD Spectra of PC, Electro spun PC/PANI, PC/EPS, PC/EPS/PANI, and PC/EPS/PANI/Zno Fibres.

3.3. Scanning electron microscopy (SEM) analysis

The morphology of 15 wt. % electrospun PC was shown in Figure 9 (a), shows a non-fibrous porous surface that is evenly distributed. Non-fibre formation may be due to the low molecular weight of polycarbonate. The SEM micrograph of 15 wt. % EPS, PC/EPS, PC/EPS/PANI, PC/EPS/PANI/ZnO were shown in Figures 9 (b)-9 (e) respectively. All the fibres of the composite of PANI as shown in Figure 9 (d) and 9 (e) were bead free with pores formation. Pores formation is due to rapid evaporation of volatile solvent causing fast phase separation in the spinning jet, which results in solvent-less and polymer-rich phases on the fibre surface [2-9]. The SEM micrographs obtained in Figure 9 (b) shows bead-less fibre with a non-porous surface while the micrograph obtained in Figure 9 (c) and (e) exhibited ribbon-like with traces of bead formation. The ribbon-like fibres obtained can be related to solvent evaporation during the electrospinning process. Beads formation on fibres may be as a result of lower polymer concentration than critical value and solution viscosity required to maintain a stable polymer jet [21]. Also, bead formation can also be attributed to high electrostatic force that attracts the polymer jet to the conductive collector.

Figure 9 (e) shows SEM micrograph of the electrospun PC/EPS/PANI/ZnO. The micrograph revealed fibres with non-porous surface. The addition of ZnO nanoparticles may result in accumulation of a higher charge density on the surface of the ejected jet during the process of electrospinning, and overall electric charges carried by the electrospinning jet significantly increased. The diameter of the resulting fibres at 15 wt. % (EPS, PC/EPS, PC/EPS/PANI and PC/EPS/PANI/ZnO) was 1.25 ± 0.05, 1.66 ± 0.31, 1.79 ± 0.50 and 3.08 ± 0.26 µm respectively.

3.4. Thermal characterization (DTA analysis)

Figure 10 presents thermographs of polycarbonate (PC) and electrospun PC (Fig. 10a); expanded polystyrene (EPS) and electrospun EPS (Fig. 10b); EPS and electrospun PC/EPS (Fig. 10c); EPS and electrospun PC/EPS/PANI (Fig. 10d); and EPS and electrospun PC/EPS/PANI/ZnO (Fig. 10e). No noticeable peaks for glass transition temperature were observed in all the samples. The melting temperatures of the used compact disc (PC) and electrospun PC were found to be 186.6°C and 220.2°C (Fig.10a) respectively. From the thermograph in Figure 10 (b), melting temperature of EPS and electro spun EPS was 244.4 °C and 261.8°C respectively.
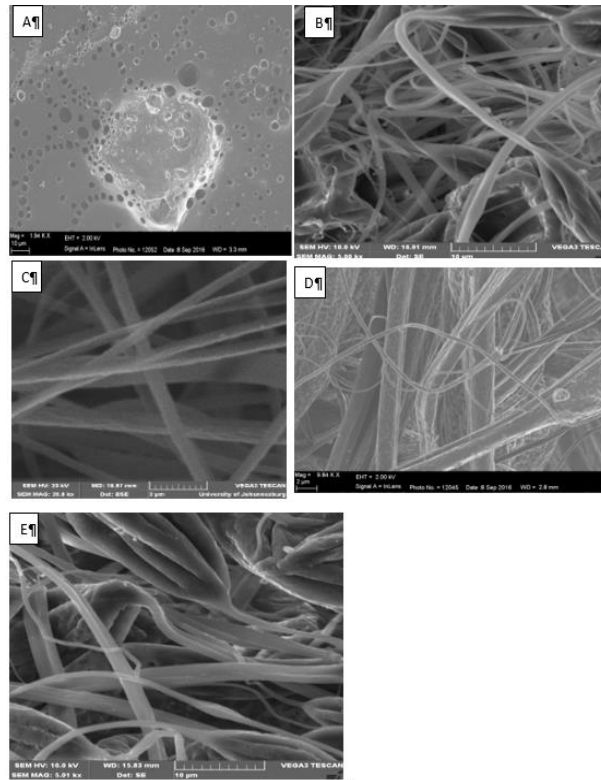
Fig. 9: SEM Micrographs of 15 Wt. % Electrospun A) PC B) EPS C) PC/EPS D) PC/EPS/PANI and E) PC/EPS/PANI/Zno.

The melting temperature of electrospun PC/EPS in Figure 10 (c) was found to be 255.1°C. With the addition of polyaniline (PANI) to the PC/EPS to form composite, melting temperature decreases to 155.4°C as shown in Figure 10 (d). Figure 10 (e) shows the DTA thermograph of PC/EPS/PANI/ZnO. It was observed that the melting temperature increases to 246.1°C. The difference in melting temperature between PC, EPS and their corresponding fibres might be due to resulting surface area per unit mass and filler effect. Fillers with low molecular mass such as ZnO act as nucleus for crystallization.

A)

B)

C)

D)

E)
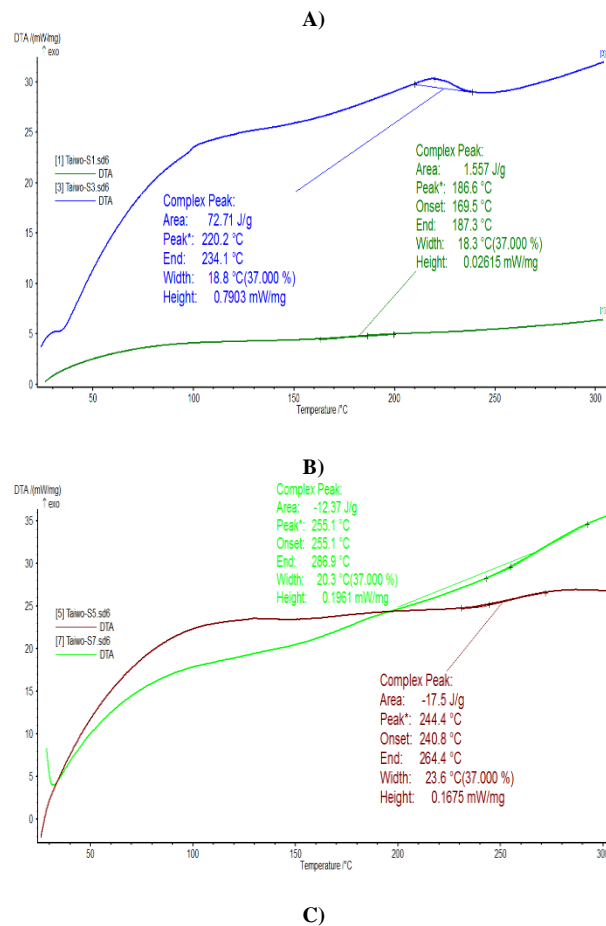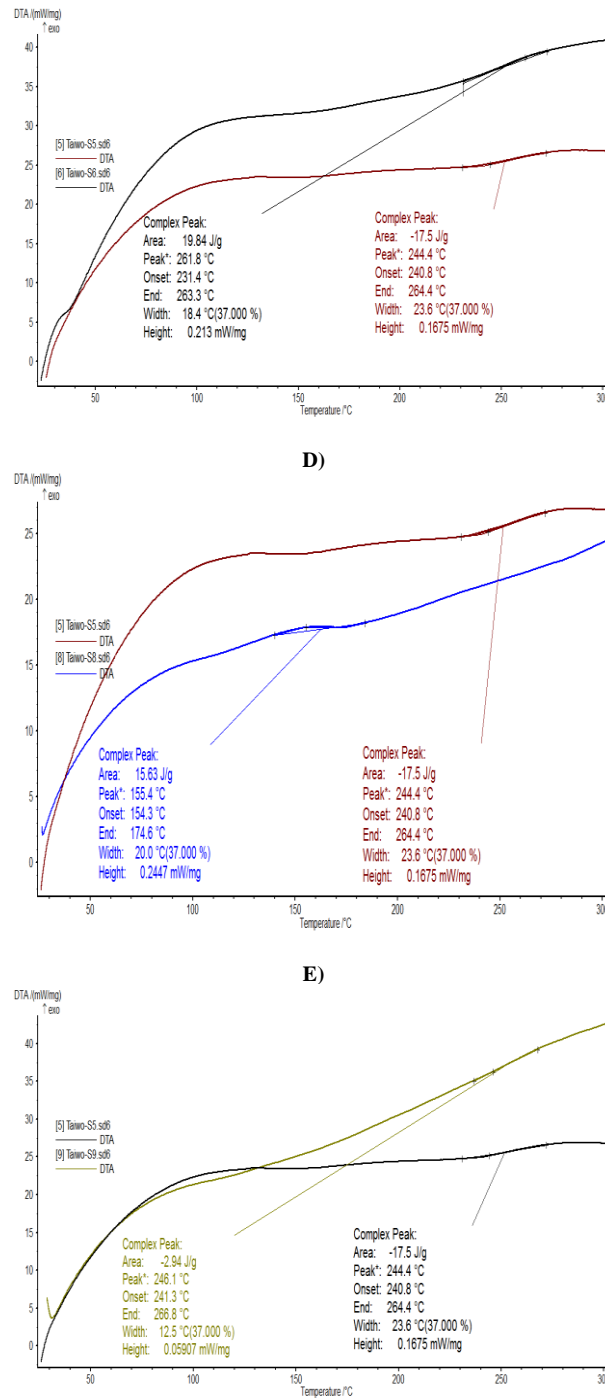
Fig. 10: DTA Curves for the A) Polycarbonate and Electro spun PC A) Expanded Polystyrene and Electro spun Expanded Polystyrene C) EPS and Electro spun PC/EPS D) EPS and E) Electro spun PC/EPS/PANI (E) EPS and Electro spun PC/EPS/PANI/ZNO.

3.5. Gas sensing response of the fibre

Figure 10a shows the sensitivity of PC/EPS/PANI/ZnO fibre with temperature. The sensitivity may be due to the presence of conducting materials such as PANI and ZnO which are dispersed across insulating carriers. The conductors interact with gas molecules resulting in a change bipolar on density inside the band gap and changes the resistance of the sensing material [18]. The sensitivity was found to be increasing gradually with temperature and attained maximum sensitivity at 25°C, then decreased at higher temperature. The decrease in sensitivity with increase in temperature may be due to non-contribution of the inorganic component of the blend to gas adsorption based. Sensitivity reduces as scaffold temperature increases, in this case polymer tends to melts at this temperature. This results into morphological damage thereby surface area to volume ratio will be alter. At 50 °C, sensitivity reduced drastically, probably due to non-available for adsorption and interaction between the adsorbed oxygen species and liquefied petroleum gas which led to the decrease in sensitivity. Figure 10b represents the response time of PC/EPS/PANI/ZnO fibre for 1000 ppm LPG. The response time is the time required for sensor to respond to a step concentration change from zero to a certain concentration value. It was observed that PC/EPS/PANI/ZnO fibre shows the highest sensitivity at ~3 seconds, indicating that the material has a good and short response time. This indicates the suitability of nanofibrous PC/EPSPANI/ZnO towards LPG sensing at room temperature.
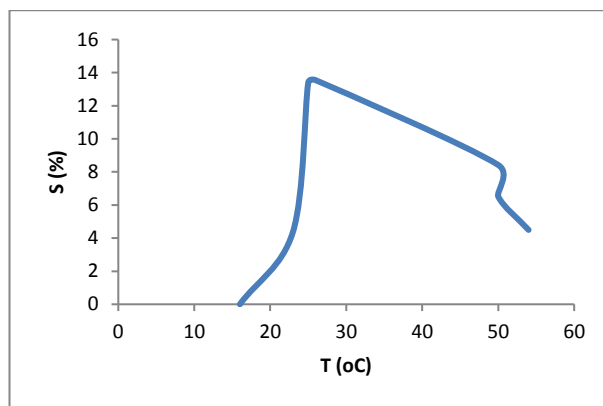
Fig. 10: A) Gas Sensing Characteristics of PC/EPS/PANI/Zno Fibre.
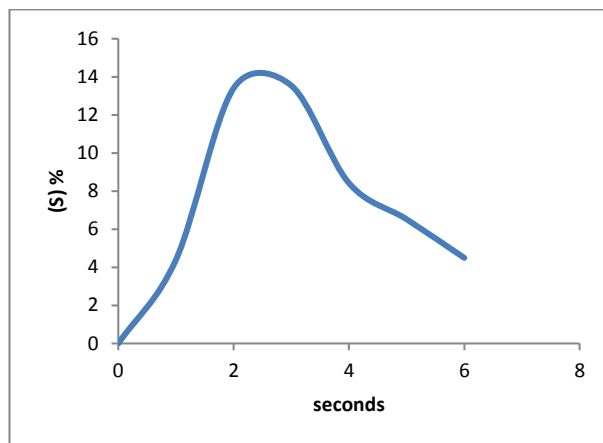
Fig. 10: B) Sensitivity Against Time of PC/EPS/PANI/Zno Fibre.

4. Conclusion

Therefore, viable potential of re-use polymer waste (unused compact disc (polycarbonate) and expanded polystyrene) is presented. We present sustainable pathway to reduce gas sensor cost, re-use polymer wastes, monitor gases at room temperature.

Acknowledgement

References

[1]   Y.L. Tharpes, International Environmental Law: Turning the Tide on Marine Pollution.U Miami Inter-Am L Rev., 20, 3 (1989), pp. 579-614.
[2]   S. O. Alayande, A.Y. Fasasi, E. O. Dare, J.A. Ajao, D. Pelemo and G. A. Osinkolu, Recycling Polystyrene through Electrospinning Technique' Nigerian Journal of Material Science and Engineering, 3, (2012), 71-75.
[3]   S. O. Alayande, The development of nanoporous membranes for crude oil sorbent and spillage remediation (PhD Thesis) Federal University of Agriculture, (2015), Abeokuta, Nigeria.
[4]   S. O. Alayande, E. O. Dare, T. A.M. Msagati A. K. Akinlabi and P.O. Aiyedun, Novel Nanoporous Sorbent as Solid Phase extraction forPetroleum Fingerprinting, Journal of Applied Physic A, 122, (2016),4, 1-7. https://doi.org/10.1007/s00339-016-9931-z.
[5]   S.O.Alayande, E. O. Dare, T.A.M. Msagati, A. K. Akinlabi, and P.O. Aiyedun, Superhydrophobic and superoleophillic surface of porous beaded electrospun polystyrene and polystyrene-zeolite fiber for crude oil-water separation, Physics and Chemistry of the Earth, 92 (2016) 7-13. https://doi.org/10.1016/j.pce.2015.10.002.
[6]   S.O.Alayande, F.O.G. Olorundare., D. Nkosi E. O. Dare, T.A.M. Msagati, B.B. Mamba Superoleophillic electrospun polystyrene/exfoliated graphite fibre for selective removal of crude oil from water. Physics and Chemistry of the Earth, 92, (2016) 3-6 https://doi.org/10.1016/j.pce.2015.09.004.
[7]   S.O. Alayande, S. Olatubosun, S. Allo, O. Adedoyin, D. Olalekan, O. Sanda, A.Fasasi, O. Dare, J. Ajao, D. Pelemo and G.A. Osinkolu, Porous and non-porous electrospun Fibres from discarded extruded polystyrene Intl. Journal of Physical Sciences, 7,11, (2012), 1832-1836. https://doi.org/10.5897/IJPS11.1783.
[8]   S.O Alayande., E.O. Dare, A.K. Akinlabi, A.Y. Fasasi and G.A. Osinkolu Nanostructuring of waste polystyrene, Journal of Chem. Soc. of Nig., 38, 2, (2013) 79-82.
[9]   J. P. Seon., S. P. Chul and Y. Hyeonseok, Chemo-Electrical Gas Sensors Based on Conducting Polymer Hybrids, Polymers *9*, (2017), 155 https://doi.org/10.3390/polym9050155.
[10] S.S. Umare, B.H. Shambharkar and R.S. Ningthoujam, Synthesis and Characterization of Polyaniline-Fe3O4 Nanocomposite: Electrical Conductivity, Magnetic, Electrochemical Studies. Synthetic Metals, 160, 17-18, (2010), 1815- 1821. https://doi.org/10.1016/j.synthmet.2010.06.015.
[11] P.K. Karin, Chemical gas sensors based on organic semiconductor polypyrrole, Crit. Rev. Anal. Chem. 32, (2002), 121–140. https://doi.org/10.1080/10408340290765489.
[12] J.J. Miasik, A. Hooper, B.C. Tofield, Conducting polymer gas sensors, J. Chem. Soc., Faraday Trans. 82, (1986), 1117–1126. https://doi.org/10.1039/f19868201117.

[13] F. Zee, J.W. Judy, Micro machined polymer-based chemical gas sensor array, Sens. Actuators B, 72, (2001), 120–128. https://doi.org/10.1016/S0925-4005(00)00638-9.

[14] H. Yoon, J. Jang, Conducting-polymer nanomaterials for high-performance sensor applications: Issues and challenges, Adv. Funct. Mater. 19, (2009), 1567–1576. https://doi.org/10.1002/adfm.200801141.

[15] H. Yoon, Current trends in sensors based on conducting polymer nanomaterials, Nanomaterials, 3, (2013) 524–549. https://doi.org/10.3390/nano3030524.

[16] X.F. Lu, W.J. Zhang, C. Wang, T.C. Wen, Y. Wei, One-dimensional conducting polymer nanocomposites: Synthesis, properties and applications. Prog. Polym. Sci. 36, (2011), 671-712. https://doi.org/10.1016/j.progpolymsci.2010.07.010.

[17] A.T. Rajesh, D. Kumar, Recent progress in the development of nano-structured conducting polymers/nanocomposites for sensor applications, Sens. Actuator B Chem. 136, (2009), 275–286. https://doi.org/10.1016/j.snb.2008.09.014.

[18] Y.S. Lee, B.S. Joo, N.J. Choi, J.O. Lim, J.S. Huh, and D.D. Lee "Visible optical sensing of ammonia based on polyaniline film, Sensors and Actuators B, 93, 1–3, (2003), 148–152. https://doi.org/10.1016/S0925-4005(03)00207-7.

[19] J. Yue, Z.H. Wang, K.R. Cromack, A.J. Epstein, A.G. MacDiarmid, Effect of sulfonic acid group on polyaniline backbone, Journal of the American Chemical Society 113, (2003), 2665–2671. https://doi.org/10.1021/ja00007a046.

[20] B. Alessio, D. Maximilian, L.N. Pierandrea, B. Piero, Synthesis and characterization of zinc oxide nanoparticles: application to textiles as UV-absorbers, J Nanopart. Res. 10, (2008), 679–689. https://doi.org/10.1007/s11051-007-9318-3.

[21] A. Frenot, I.S. Chronakis, Polymer nanofibers assembled by electrospinning, Current Opinion in Colloid & Interface Science, 8, (2003), 64-75. https://doi.org/10.1016/S1359-0294(03)00004-9.